Nuclear Medicine and Biology 42 (2015) 19–27

Contents lists available at ScienceDirect

Nuclear Medicine and Biology

journal homepage: www.elsevier.com/locate/nucmedbio

D-amino acid peptide residualizing agents bearing *N*-hydroxysuccinimido- and maleimido-functional groups and their application for trastuzumab radioiodination

Marek Pruszynski [a,1], Eftychia Koumarianou [a], Ganesan Vaidyanathan [a], Satish Chitneni [a], Michael R. Zalutsky [a,b,*]

[a] Department of Radiology, Duke University Medical Center, Durham, NC, USA
[b] Departments of Biomedical Engineering and Radiation Oncology, Duke University, Durham, NC, USA

ARTICLE INFO

Article history:
Received 4 August 2014
Accepted 7 August 2014

Keywords:
Radioiodination
Trastuzumab
Radionuclide therapy
D-amino acid peptide
Residualizing agents

ABSTRACT

Introduction: Proteins that undergo receptor-mediated endocytosis are subject to lysosomal degradation, requiring radioiodination methods that minimize loss of radioactivity from tumor cells after this process occurs. To accomplish this, we developed the residualizing radioiodination agent N^{ϵ}-(3-[*I]iodobenzoyl)-Lys^5-N^{α}-maleimido-Gly^1-D-GEEEK (Mal-D-GEEEK-[*I]IB), which enhanced tumor uptake but also increased kidney activity and necessitates generation of sulfhydryl moieties on the protein. The purpose of the current study was to synthesize and evaluate a new D-amino acid based agent that might avoid these potential problems.
Methods: N^{α}-(3-iodobenzoyl)-(5-succinimidyloxycarbonyl)-D-EEEG (NHS-IB-D-EEEG), which contains 3 D-glutamates to provide negative charge and a *N*-hydroxysuccinimide function to permit conjugation to unmodified proteins, and the corresponding tin precursor were produced by solid phase peptide synthesis and subsequent conjugation with appropriate reagents. Radioiodination of the anti-HER2 antibody trastuzumab using NHS-IB-D-EEEG and Mal-D-GEEEK-IB was compared. Paired-label internalization assays on BT474 breast carcinoma cells and biodistribution studies in athymic mice bearing BT474M1 xenografts were performed to evaluate the two radioiodinated D-peptide trastuzumab conjugates.
Results: NHS-[^{131}I]IB-D-EEEG was produced in 53.8% ± 13.4% and conjugated to trastuzumab in 39.5% ± 7.6% yield. Paired-label internalization assays with trastuzumab-NHS-[^{131}I]IB-D-EEEG and trastuzumab-Mal-D-GEEEK-[^{125}I]IB demonstrated similar intracellular trapping for both conjugates at 1 h (^{131}I, 84.4% ± 6.1%; ^{125}I, 88.6% ± 5.2%) through 24 h (^{131}I, 60.7% ± 6.8%; ^{125}I, 64.9% ± 6.9%). In the biodistribution experiment, tumor uptake peaked at 48 h (trastuzumab-NHS-[^{131}I]IB-D-EEEG, 29.8% ± 3.6%ID/g; trastuzumab-Mal-D-GEEEK-[^{125}I]IB, 45.3% ± 5.3%ID/g) and was significantly higher for ^{125}I at all time points. In general, normal tissue levels were lower for trastuzumab-NHS-[^{131}I]IB-D-EEEG, with the differences being greatest in kidneys (^{131}I, 2.2% ± 0.4%ID/g; ^{125}I, 16.9% ± 2.8%ID/g at 144 h).
Conclusion: NHS-[^{131}I]IB-D-EEEG warrants further evaluation as a residualizing radioiodination agent for labeling internalizing antibodies/fragments, particularly for applications where excessive renal accumulation could be problematic.

1. Introduction

Human epidermal growth factor receptor type 2 (HER2 or ErbB2) is overexpressed in 20%–30% of breast cancers as well as in a subset of ovarian carcinomas, non-small cell lung cancers, gastric and colon cancers [1]. Novel medicaments targeting HER2 based on the monoclonal antibodies (mAbs) trastuzumab and pertuzumab, and tyrosine kinase inhibitors such as lapatinib have been developed and shown significant therapeutic benefit in patients with HER2-expressing malignancies [2–4]. Moreover, these mAbs and their fragments have been evaluated in preclinical and clinical studies as potential carriers of radionuclides for diagnostic and therapeutic applications [5–9].

With regard to utilizing HER2-specific mAbs for targeting radionuclides to tumors, an attractive feature of a radioiodination strategy is the availability of iodine radionuclides with diverse decay characteristics. In principle, this allows the same molecular structure and labeling chemistry to be employed for different applications including SPECT (^{123}I) and PET (^{124}I) imaging as well as β^--particle (^{131}I) and Auger electron (^{123}I, ^{125}I) targeted radiotherapy. However, direct radioiodination of tyrosine residues is not a suitable method for labeling internalizing mAbs such as trastuzumab due to rapid loss of

* Corresponding author at: Duke University Medical Center, Box 3808, Durham, NC, USA. Tel.: +1 919 684 7708; fax: +1 919 684 7121.
E-mail address: zalut001@mc.duke.edu (M.R. Zalutsky).
[1] Present address: Institute of Nuclear Chemistry and Technology, Warsaw, Poland.

http://dx.doi.org/10.1016/j.nucmedbio.2014.08.007
0969-8051/

radioactivity from tumor cells after lysosomal degradation of the labeled protein [10]. This problem can be circumvented by the use of residualizing agents, which generate radiolabeled catabolites that are trapped within tumor cells after mAb degradation. Our approach for developing residualizing agents for the radioiodination of internalizing mAbs has focused on charged prosthetic groups, which yield labeled catabolites that are poorly transported across lysosomal/cell membranes [11–14]. One of the most promising reagents derived from this strategy is N^{ϵ}-(3-[*I]iodobenzoyl)-Lys^5-N^{α}-maleimido-Gly^1-D-GEEEK (Mal-D-GEEEK-[*I]IB) [15,16]. Labeling of internalizing intact mAbs and fragments with Mal-D-GEEEK-[*I]IB increased tumor retention of radioiodine by up to 4-fold compared with xenograft radioiodine accumulation levels observed when these proteins were labeled by direct radioiodination using Iodogen.

Because this prosthetic group contains a maleimide functionality, it requires generation of free sulfhydryl groups on the protein to allow the coupling reaction to proceed [15]. Treating the protein with 2-iminothiolane (Traut's reagent) is the most widely used technique for generating sulfhydryl groups and offers the advantage compared with constituent disulfide bond reduction of less disruption of protein tertiary structure [16]. Generation of sulfhydryl groups on protein generally is best performed just before reaction with the radiolabeled maleimide to avoid formation of multimeric species resultant from their oxidation back to disulfides. However, the overall time for preparation and purification of thiol-derivatized mAb, and its coupling to the radiolabeled maleimide can be up to 4 h, which is not ideal, particularly if routine use shorter-lived ^{123}I ($t_{1/2}$ = 13.2 h) or ^{211}At ($t_{1/2}$ = 7.2 h) is envisioned. On the other hand, utilization of prosthetic groups containing active NHS esters allows much faster conjugation to the lysine residues of unmodified proteins under mild conditions, an approach used successfully in the past with other residualizing agents [11,13,14].

The objective of the current study was to synthesize a new residualizing agent, analogous to Mal-D-GEEEK-[*I]IB but bearing a NHS ester to facilitate its conjugation with proteins. The usefulness of this reagent for labeling trastuzumab was investigated. In addition, trastuzumab labeled with these two residualizing agents was compared in HER2-expressing human breast carcinoma cell and xenograft models to evaluate linkage-dependent effects on *in vitro* and *in vivo* behavior.

2. Materials and methods

2.1. General

All chemicals of pure reagent grade quality were purchased from Sigma-Aldrich (St. Louis, MO) unless otherwise specified. All reagents used in cell culture studies were purchased from Invitrogen except where noted. No-carrier-added Na^{125}I and Na^{131}I in 0.1 M NaOH with specific activities of 2200 Ci/mmol and 1200 Ci/mmol, respectively, were purchased from Perkin-Elmer Life and Analytical Sciences (Boston, MA). Trastuzumab (Herceptin®, Genentech, San Francisco, CA), obtained from the Duke Cancer Institute pharmacy, was purified from excipients by ultrafiltration on a micro-spin column with a 100 kDa cut-off membrane, transferred to adequate volumes of phosphate buffer pH 8.0 or borate buffer pH 8.5 and stored frozen. A Mal-D-GEEEK-IB standard and the corresponding tin precursor N^{ϵ}-(3-(tri-*n*-butylstannyl)benzoyl)-Lys^5-N^{α}-maleimido-Gly^1-D-GEEEK (Mal-D-GEEEK-TB) were synthesized as reported before [15]. Bis-*N*-hydroxysuccinimidyl 5-iodo-isophthalate and bis-*N*-hydroxysuccinimidyl 5-(tri-*n*-butylstannyl)isophthalate were prepared as reported [17]. Fmoc-Gly-Wang resin and Fmoc-D-Glu-(O*t*Bu)-OH were obtained from Novabiochem (West Chester, PA).

Solid-phase peptide synthesis was carried out on a Perkin-Elmer Applied Biosystems (Foster City, CA) model 433A automated peptide synthesizer employing their Fast-Moc chemistry with HBTU activation of carboxyl groups. Mass spectra were recorded using an Agilent 1100 LC/MSD Trap for electrospray ionization (ESI) LC-MS. High-pressure liquid chromatography (HPLC) was performed using the following systems: (1) for analytical and semi-preparative HPLC of nonradioactive compounds, a Waters Model Delta 600 semi-prep system with a Model 600 controller and a Model 2487 dual wavelength absorbance detector; data were acquired using Millenium software; and (2) for radiochemical HPLC separations, a Beckman Gold HPLC system equipped with a Model 126 programmable solvent module coupled with a Model 166 NM variable wavelength detector and a Model 170 radioisotope detector; data were acquired using 32 Karat software. A Waters XTerra C18 HPLC column (4.6 × 250 mm, 5 μm), eluted at a flow rate of 1 mL/min was used for analytical and radioanalytical chromatography and a Waters Xterra C18 column (19 × 150 mm, 7 μm), eluted at 10 mL/min was used for semi-preparative chromatography. The gradient elution system consisted of deionized water (A) and acetonitrile (B), both containing 0.1% acetic acid (v/v). Solvents for HPLC were obtained as HPLC grade and degassed by ultrasonication for 15–20 min just before use. The following two gradient conditions were employed: (I) the proportion of B was increased linearly from 50% to 100% over a period of 30 min; (II) the proportion of B was held at 4% for 10 min and then linearly increased to 100% in the next 30 min.

2.2. Synthesis

2.2.1. D-EEEG (**2**)

Three side chain protected (O*t*Bu) D-glutamic acid molecules were sequentially attached to glycine supported on Wang resin (0.1 mmol) using the automated synthesizer and Fmoc chemistry. The removal of the Fmoc group on the last D-glutamic acid was achieved by treatment with 20% piperidine in dimethylformamide (DMF) followed by several washes. Finally, the tetrapeptide was cleaved from the resin by treatment with 100:95:2.5:2.5 (v/v/v/v) dichloromethane:trifluoroacetic acid:water:triisopropyl-silane. The resin was filtered, and the peptide was precipitated from the concentrated filtrate with the addition of diethyl ether. Analytical HPLC conditions/gradient I: t_R = 3.1 min. MS (*m/z*) Calcd. for: $C_{17}H_{26}N_4O_{11}$ 462.2. Found: 463.1 $(M + H)^+$.

2.2.2. NHS-IB-D-EEEG (**3**)

A solution of D-EEEG (10.0 mg; 21.6 μmol) in 200 μL DMF was added to a solution of bis-*N*-hydroxysuccinimidyl 5-iodo-isophthalate (47.2 mg; 97.1 μmol) in 200 μL of 2% (v/v) triethylamine in DMF over a period of 20 min, and the homogenous mixture was stirred overnight under argon atmosphere at room temperature. The peptide was precipitated with excess cold ether, pelleted, washed several times with cold ether, and purified by preparative HPLC using conditions I to obtain a white powder 8.2 mg (45.5%). Analytical HPLC conditions (gradient I): t_R = 10.0 min. MS (*m/z*) Calcd. for: $C_{29}H_{32}IN_5O_{16}$ 833.1. Found: 834.2 $(M + H)^+$.

2.2.3. NHS-TB-D-EEEG (**4**)

A solution of D-EEEG (46.2 mg; 100 μmol) in 1.0 mL DMF was added to a solution of bis-*N*-hydroxysuccinimidyl 5-(tri-*n*-butylstannyl) isophthalate (236.2 mg; 363.8 μmol) in 1.5 mL of 2% (v/v) triethylamine in DMF over a period of 30 min. After stirring the homogenous mixture overnight under argon atmosphere at room temperature, the peptide was isolated and purified as above to get 12.4 mg (12.4%). Analytical HPLC conditions (gradient I): t_R = 13.0 min. MS (*m/z*) Calcd. for: $C_{41}H_{59}N_5O_{16}Sn$ 997.3. Found: 998.4 $(M + H)^+$.

2.3. Radiochemistry

2.3.1. NHS-[^{131}I]IB-D-EEEG

Acetic acid (AcOH; 40 μL) was added to a ½-dram vial containing dried sodium [^{131}I]iodide (3.2–5.2 mCi; 7–12 μL in 0.1 M NaOH) followed by NHS-TB-D-EEEG (80 μg/25 μL AcOH) and *N*-chlorosuccinimide (0.4 mg/20 μL AcOH). The mixture was incubated for 15 min, and the labeled peptide was isolated by reversed-phase analytical HPLC

(gradient II); $t_R = 28.9$ min. The HPLC fractions containing the product were collected; most of the acetonitrile was removed using an argon stream and concentrated by solid-phase extraction using a Waters Sep-pak classic C18 cartridge (Milford, MA). NHS-[^{131}I]IB-D-EEEG was eluted from the solid-phase cartridge with 1 mL of 1% AcOH in anhydrous acetonitrile, and the solvents from the eluate evaporated to dryness using a stream of argon. The residual radioactivity was used as such for coupling to trastuzumab.

2.3.2. Mal-D-GEEEK-[^{125}I]IB

The trialkylstannyl precursor was radioiodinated and purified by reversed-phase HPLC as reported before [15,18]. Briefly, 40 μL of AcOH was added to dried sodium [^{125}I]iodide (4.0–5.5 mCi; 12–20 μL in 0.1 M NaOH) followed by Mal-D-GEEEK-TB (50 μg/25 μL AcOH) and *N*-chlorosuccinimide (0.4 mg/20 μL AcOH). After 15 min incubation, Mal-D-GEEEK-[^{125}I]IB was isolated by analytical HPLC using conditions II; $t_R = 29.5$ min. The HPLC fractions containing the product were concentrated on a Sep-pak cartridge as described above and the labeled peptide eluted from the cartridge using 1 mL of anhydrous methanol. After evaporation of methanol, the residual radioactivity was used as such for conjugation to trastuzumab.

2.4. Trastuzumab labeling

2.4.1. NHS-[^{131}I]IB-D-EEEG

A solution of trastuzumab (154 μL; 200 μg; 1.3 mg/mL) in 0.1 M borate buffer, pH 8.5, was added to dried NHS-[^{131}I]IB-D-EEEG (580–1400 μCi) in a ½-dram vial, vortexed and incubated at room temperature for 20 min. The labeled mAb conjugate was isolated by gel filtration on a PD-10 column (GE Healthcare, Piscataway, NJ) eluted with PBS, pH 7.4. For determination of K_D, trastuzumab was labeled in similar fashion using NHS-[^{125}I]IB-D-EEEG.

2.4.2. Mal-D-GEEEK-[^{125}I]IB

Trastuzumab was first treated with 2-iminothiolane (Traut's reagent, Thermo Scientific) to generate free sulfhydryl groups as reported previously [18]. Briefly, 2-iminothiolane (2.8 μL; 2 mg/mL) in 0.1 M phosphate buffer (PB), pH 8.0 containing 5 mM EDTA, was added to an Eppendorf tube containing trastuzumab (154 μL; 200 μg; 1.3 mg/mL) in the same buffer, and the tube vortexed and left at room temperature for 90 min. The thiol-derivatized mAb was isolated using a micro-spin G-25 column (GE Healthcare, Piscataway, NJ) equilibrated with 0.1 M PB, pH 7.0, containing 5 mM EDTA. The isolated thiolated trastuzumab was added to a ½-dram vial containing dried Mal-D-GEEEK-[^{125}I]IB (730–1900 μCi) and the mixture incubated at room temperature for 45 min with occasional vortexing. The reaction was quenched by incubation for 15 min with iodoacetamide (10 μL; 100 mg/mL in PB/EDTA pH 7.0). The radiolabeled mAb was purified on a PD-10 column as described above.

2.5. Characterization of labeled mAbs

Protein-associated radioactivity was determined by instant thin layer chromatography (ITLC) with PBS as the mobile phase and by co-precipitation with human serum albumin (HSA) using 20% trichloroacetic acid (TCA). The immunoreactive fraction of the radiolabeled mAb conjugates was determined by a modified Lindmo method using magnetic beads coated with recombinant ErbB2/HER2 extracellular domain, or as a nonspecific control, BSA [18]. Radiolabeled mAbs were also analyzed by SDS-PAGE under non-reducing conditions as described [18]. Radioactivity distributions on the gels were measured using a Storage Phosphor System Cyclone Plus (Perkin-Elmer Life and Analytical Sciences, Downers Grove, IL) and analyzed using Optiquant software (version 5.0) provided by the manufacturer.

2.6. Binding affinity and internalization assays

HER2-expressing BT474 human breast carcinoma cells were grown in DMEM/F12 medium supplemented with 10% fetal calf serum, streptomycin (100 μg/mL), and penicillin (100 IU/mL) at 37 °C in 5% CO_2. Medium was changed every two days and cells passaged by trypsinization (0.05% Trypsin-EDTA) when they were about 80% confluent. For the determination of binding affinity, BT474 cells were seeded in 24 well plates (8×10^4 cells/well) and incubated with increasing concentrations of trastuzumab-NHS-[^{125}I]IB-D-EEEG or trastuzumab-Mal-D-GEEEK-[^{125}I]IB (0.05–100 nM), each in triplicate, at 4 °C for 2 h; to determine nonspecific binding, the assay was repeated with a 100-fold excess of trastuzumab in the wells. Cell-associated radioactivity was determined as reported before [18], and K_D values were calculated using GraphPad Prism software. Paired-label internalization assays were performed in 6 well plates (8×10^5 cells/well), at final concentration 5×10^{-9} nM for both labeled mAb conjugates, with non-specific uptake determined by co-incubation with a 100-fold excess of trastuzumab. The cells were incubated at 4 °C for 1 h, unbound radioactivity was removed, and the cells incubated with fresh medium at 37 °C for various time points up to 24 h. The percentages of initially bound radioactivity that was internalized, membrane-bound, and that present in the cell culture supernatants were determined as described [18]. The fraction of radioactivity in the cell culture supernatants that was protein-associated was determined by TCA precipitation. Radioactivity levels were measured on a dual-channel 1480 Automated Gamma Counter (Perkin-Elmer Life and Analytical Sciences, Downers Grove, IL).

2.7. Paired-label biodistribution

Animal studies were performed under guidelines established by the Duke University Institutional Animal Care and Use Committee. To augment tumor growth, 60-day continuous release 17-β-estradiol pellets (Innovative Research of America, Sarasota, FL) were implanted on the back of 10–12 week old female NOD.CB17-*Prkdc*^{scid}/J mice (Jackson Laboratories, Bar Harbor, ME). Two days later, mice were inoculated in the flank with 5×10^6 BT474M1 cells in 50% Matrigel (BD Biosciences, Bedford, MA). Biodistribution studies were initiated when tumors reached a volume of 350–500 mm^3. Six groups of 5 mice were injected *via* the tail vein with 1.1 μCi (0.8 μg) of trastuzumab-NHS-[^{131}I]IB-D-EEEG and 5 μCi (0.8 μg) of trastuzumab-Mal-D-GEEEK-[^{125}I]IB. At 4, 12, 24, 48, 96 and 144 h post injection, mice were euthanized by isofluorane overdose, dissected, and organs isolated. Blot-dried tissues of interest were weighed and counted for ^{125}I and ^{131}I radioactivity along with injection standards in a dual-channel gamma counter. Results were expressed as percentage of injected dose per gram of tissue (%ID/g), except for thyroid for which %ID/organ values was determined. Tumor-to-tissue ratios also were calculated.

2.8. Statistical analysis

Data are presented as mean ± SD. The statistical significance of differences in uptake between the two tracers was determined by a paired 2-tailed Student *t*-test using Microsoft Excel. A *P* value less than 0.05 was considered statistically significant.

3. Results and discussion

3.1. Chemical and radiochemical synthesis

The NHS-IB-D-EEEG standard and its corresponding tin precursor were synthesized as depicted in Scheme 1. The peptide D-EEEG (**2**), obtained by solid-phase peptide synthesis and subsequent cleavage, was conjugated with bis-*N*-hydroxysuccinimidyl 5-iodo-isophthalate and bis-*N*-hydroxysuccinimidyl 5-(tri-*n*-butylstannyl)isophthalate

to render the standard **3** and the tin precursor **4**, respectively, in moderate yields. The molecular weights found by mass spectrometry for the tetrapeptide D-EEEG, as well as these iodo and tin derivatives, were consistent with theoretically calculated values.

The tin precursor **4** was radioiodinated to provide NHS-[^{131}I]IB-D-EEEG ([^{131}I]**3**; Scheme 1) in 53.8% ± 13.4% (n = 6) yield and 96.8% ± 2.6% radiochemical purity. The efficiency for coupling NHS-[^{131}I]IB-D-EEEG to trastuzumab was 39.5% ± 7.6% (n = 4). In comparison, Mal-D-GEEEK-[^{125}I]IB was synthesized from its tin precursor in 81.7% ± 11.3% (n = 6) yield and 97.7% ± 1.4% radiochemical purity. Conjugation of this labeled maleimide to trastuzumab was achieved in 58.9% ± 13.0% (n = 4) yields. The lower yields for NHS-[^{131}I]IB-D-EEEG compared to Mal-D-GEEEK-[^{125}I]IB conjugation to trastuzumab might be due to several factors. The maleimide functional group in Mal-D-GEEEK-[^{125}I]IB is generally stable in aqueous solutions, whereas the *N*-hydroxysuccinimide group in NHS-[^{131}I]IB-D-EEEG is more susceptible to hydrolysis. Because water was a component of the mobile phase used for HPLC purification and subsequent solid phase extraction, hydrolysis of NHS could have occurred, which would interfere with coupling to the mAb. Coupling of NHS-activated compounds to primary amines is usually performed in slightly basic conditions such as the pH 8.5 borate buffer used in the current study. While this pH shifts the equilibrium of lysine side chain amino groups more towards the free amine *versus* the protonated form, accelerating the conjugation reaction, it also can facilitate the hydrolysis of NHS, which will decrease conjugation efficiency [19]. If higher conjugation efficiencies are needed in future studies with NHS-[^{131}I]IB-D-EEEG, a simple strategy that we have used in the past with other NHS ester radiohalogenation agents is to increase the concentration of the protein from the ~1 mg/mL used here to at least 5 mg/mL [20,21]. This increases the competition between protein coupling and hydrolysis, which can result in about a twofold higher yield for protein conjugation.

The specific activities of the labeled mAbs prepared in this study were 1.4–1.8 mCi/mg for trastuzumab-NHS-[^{131}I]IB-D-EEEG and 1.8–6.2 mCi/mg for trastuzumab-Mal-D-GEEEK-[^{125}I]IB, with higher specific activities likely obtainable, if needed, by starting with higher initial radioactivity levels. The ITLC and TCA precipitation assays indicated that ≥95% of the radioiodine activity was protein associated for both conjugates. This was in good agreement with SDS-PAGE analysis, which indicated that 94.9% ± 4.7% and 92.2% ± 5.1% (n = 2) of the radioactivity for trastuzumab-NHS-[^{131}I]IB-D-EEEG and trastuzumab-Mal-D-GEEEK-[^{125}I]IB, respectively, was present in a band with a molecular weight of about 150 kDa molecular weight, corresponding to monomeric IgG. No evidence of aggregate formation was detected.

3.2. Immunoreactive fraction and binding affinity

A potential advantage of NHS-[*I]IB-D-EEEG compared with Mal-D-GEEEK-[*I]IB is the possibility of offering higher immunoreactivity and binding affinity as a consequence of less modification of mAb. The NHS derivative modifies lysine residues directly; in contrast, with the maleimido agent, where lysine residues are first modified with Traut's reagent to generate sulfhydryl groups to react with the maleimido moiety of Mal-D-GEEEK-[*I]IB. Given that the number of lysines modified by 2-iminothiolane conjugation is greater than the number of labeled prosthetic groups coupled to the mAb [12,15], the degree of

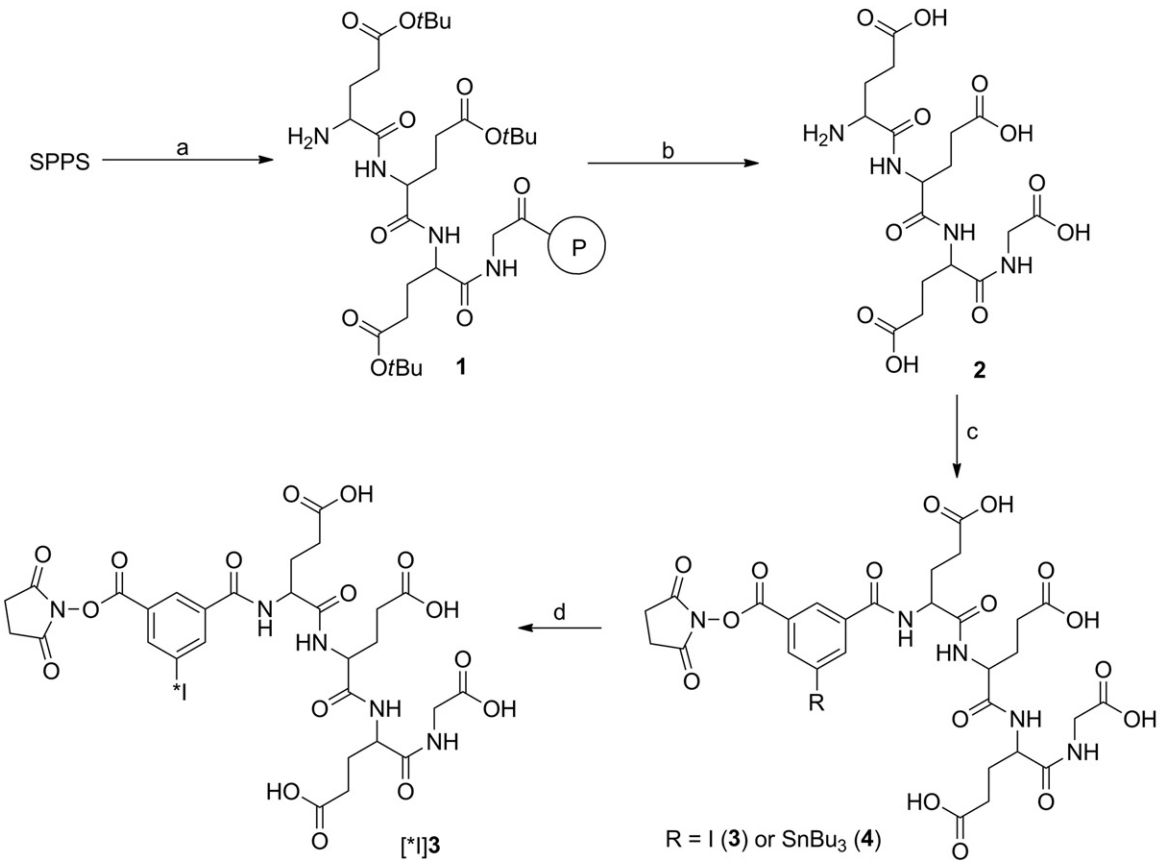

Scheme 1. Syntheses of NHS-IB-D-EEEG and its corresponding tin precursor. a) solid-phase pedtide synthesis (SPPS); b) TFA cleavage cocktail; c) bis-*N*-hydroxysuccinimidyl 5-iodo-isophthalate or bis-*N*-hydroxysuccinimidyl 5-(tri-*n*-butylstannyl)isophthalate; d) 4, radioiodine, NCS, acetic acid.

mAb modification is greater in terms of both the number of lysines modified, and when labeled, the size of the modification that is generated. Thus, one might expect higher immunoreactivity for the antibody labeled using NHS-[*I]IB-D-EEEG. However, the immunoreactive fractions determined for trastuzumab-NHS-[^{131}I]IB-D-EEEG and trastuzumab-Mal-D-GEEEK-[^{125}I]IB were 93.9% ± 3.0% and 92.0% ± 1.6% (n = 2), respectively, indicating no significant advantage for the NHS-coupled reagent. These data indicate that binding affinity of the trastuzumab to HER2 was not affected by the chemical modifications associated with the labeling. Binding affinity was evaluated using the HER2-expressing BT474 human breast carcinoma cell line. The dissociation constant (K_D) measured for trastuzumab-NHS-[^{125}I]IB-D-EEEG and trastuzumab-Mal-D-GEEEK-[^{125}I]IB was 5.4 ± 0.7 nM and 5.7 ± 0.6 nM, respectively (Fig. 1), a value similar to that of reported for trastuzumab directly radioiodinated with ^{131}I using Iodogen (2.12 nM) for the same cell line and for unlabeled trastuzumab (4.09 nM) from assays using BT474 cells [22]. These K_D values suggest that both prosthetic groups modify lysines on trastuzumab in regions not directly involved in HER2 interaction. Although NHS-[*I]IB-D-EEEG does not offer any advantage compared with Mal-D-GEEEK-[*I]IB in terms of HER2 binding of trastuzumab after labeling, it remains to be ascertained whether this is the case for other mAbs and smaller mAb fragments, which might be more susceptible to structural alteration.

3.3. Internalization and cellular processing

NHS-[*I]IB-D-EEEG, like its analogous maleimido-containing acylation agent Mal-D-GEEEK-[*I]IB, was designed as a residualizing agent based on the hypothesis that a proteolytically inert D-peptide with three negatively charged amino acids would not be transported across lysosomal and cell membranes. Paired-label internalization studies were performed to directly compare the intracellular retention and cellular processing of trastuzumab-NHS-[^{131}I]IB-D-EEEG to that of co-incubated trastuzumab-Mal-D-GEEEK-[^{125}I]IB in BT474 cells (Fig. 2). HER2-specificity of mAb uptake was confirmed by co-incubation with a 100-excess of non-labeled trastuzumab, which demonstrated that non-specific uptake was less than 0.1% of added activity at all time points. As shown in Fig. 2A, the percentage of initially bound radioactivity that was internalized within the cells was quite similar for both radionuclides throughout the 24 h observation period. For example, intracellular activity values were 84.4% ± 6.1% for trastuzumab-NHS-[^{131}I]IB-D-EEEG and 88.6% ± 5.2% for trastuzumab-Mal-D-GEEEK-[^{125}I]IB at 1 h, declining to 60.7% ± 6.8% and 64.9% ± 6.9% at 24 h. The decrease in intracellularly retained radioactivity with time observed for trastuzumab labeled using these two prosthetic groups is somewhat contradictory to the behavior seen earlier when other mAbs and mAb fragments were radioiodinated with Mal-D-GEEEK-[*I]IB. A steady increase in intracellularly retained radioactivity was observed over 24 h in internalization studies performed with an anti-EGFRvIII mAb L8A4 [15] or a double mutant fragment of trastuzumab [16] in other cell lines. With an anti-HER2 nanobody and BT474M1 cells, a fairly constant level of internalized radioactivity was observed throughout the 24 h time period [18,23].

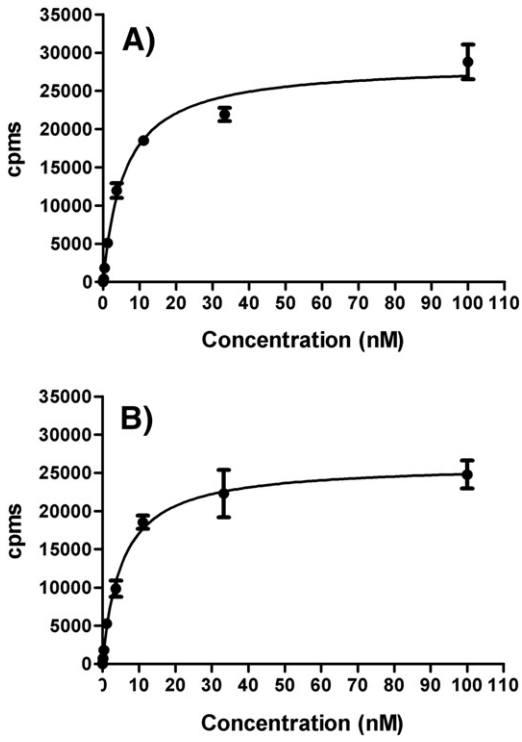

Fig. 1. Representative binding affinity curves for trastuzumab-NHS-[^{125}I]IB-D-EEEG (A) and trastuzumab-Mal-D-GEEEK-[^{125}I]IB (B) to the HER2-expressing human breast carcinoma cell line BT474.

As for the differences between the current results and those observed in previous studies with Mal-D-GEEEK-[*I]IB, the fact that different biomolecules and tumor cell lines were used might have contributed to differences in internalization and cellular retention of labeled entities generated after receptor binding of the mAbs/mAb fragments. One explanation for the slow decrease in intracellular radioactivity with time may be recycling of mAb-receptor complex back to the cell surface before it had been subjected to lysosomal proteolysis and labeled catabolite trapping. This recycling process has been demonstrated in studies with radiolabeled DOTA-Tyr^3-octreotate and somatostatin receptors [24], EGF-EGFR [25] and of direct relevance to the current work, trastuzumab-HER2 complexes [26]. As shown in Fig. 2C, the fraction of radioactivity released into cell culture supernatants increased slowly from 13.1% ± 3.9% at 1 h to 28.0% ± 4.2% at 24 h for NHS-[^{131}I]IB-D-EEEG and from 9.3% ± 3.2% to 22.8% ± 4.3% for Mal-D-GEEEK-[^{125}I]IB. TCA-soluble (non-protein associated) radioactivity released into the cell culture media increased from 1 h to 24 h from 5.5% ± 2.1% to 16.5% ± 1.4% for NHS-[^{131}I]IB-D-EEEG and from 9.9% ± 2.2% to 23.8% ± 2.5% for Mal-D-GEEEK-[^{125}I]IB (Fig. 2D). The presence of an increasing level of radioiodine activity in cell culture media, most of which is protein associated, is consistent with the release of trastuzumab-HER2 complexes from the cell but also could reflect the presence of free trastuzumab which for some reason, did not rebind to cell surface HER2. Differentiation of these two species was not done in these experiments but will be evaluated in future studies as we have done in the past with other potential residualizing agents [14]. It is worth noting that the levels of non-protein associated radioiodine in cell culture media were significantly lower ($P < 0.05$) for trastuzumab labeled using NHS-[^{131}I]IB-D-EEEG, which might be somewhat surprising given that the intracellular trapping of radioiodine was not significantly different for the two reagents. One can only speculate that this difference might represent a low degree of catabolism of trastuzumab-NHS-[^{131}I]IB-D-EEEG or its HER2 complex either on the cell surface or in the cell culture media.

Despite the decrease in intracellular radioactivity seen at later time points, it is important to point out that the degree of intracellular retention of radioactivity observed with trastuzumab labeled with NHS-[^{131}I]IB-D-EEEG or Mal-D-GEEEK-[^{125}I]IB was considerably higher than those reported for trastuzumab radioiodinated by other methods [27–29]. For example, with trastuzumab labeled with *N*-succinimidyl *p*-[^{125}I]iodobenzoate (P[^{125}I]IB), there was about 70% of internalized radioactivity in SKBR-3 cells at 1 h that decreased almost threefold to only 24.3% after 20 h incubation at 37 °C [29]. Likewise, with P[^{125}I]IB-trastuzumab, less than 12% of radioiodine activity remained internalized in NCI-N87 cells after a 24 h incubation period [28]. Consistent with these results, although P[^{125}I]IB, like the *IB moiety in the residualizing agents reported herein, is resistant to dehalogenation, it does not include structural motifs designed for

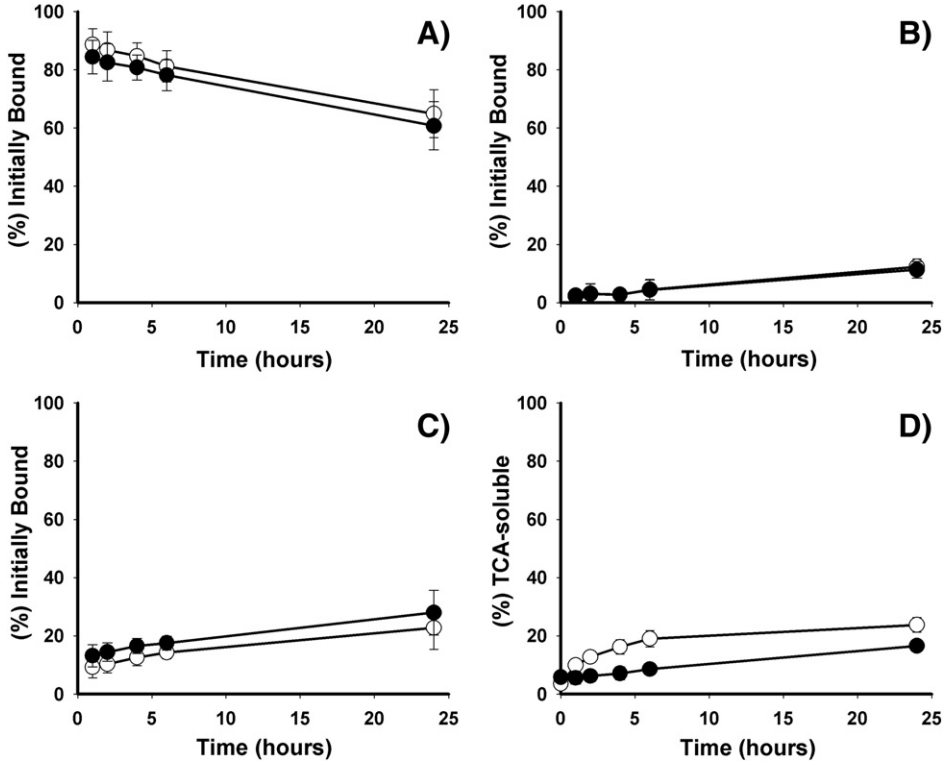

Fig. 2. Paired-label internalization and cellular processing of trastuzumab-NHS-[^{131}I]IB-D-EEEG (filled circles) and trastuzumab-Mal-D-GEEEK-[^{125}I]IB (open circles) in BT474 cells. Data are presented as the percentage of initially bound radioactivity that was internalized (A), membrane-bound (B), and present in the cell culture supernatants (C). The percentages of radioactivity leaked into the cell culture media that was TCA-soluble at various time points are also shown (D). Mean values from two independent experiments, each in triplicate, are presented with error bars represent the standard deviation.

being trapped inside cells after mAb internalization. Finally, labeling mAbs with radiometals *via* bifunctional chelates is generally considered to be an effective residualizing labeling strategy, at least in comparison with direct radioiodination [30]. Considering this, it is interesting to note that ^{111}In-DTPA-trastuzumab showed about 50% internalization at 24 h in SKOV-3 cells [31], a value somewhat lower than obtained with trastuzumab labeled using NHS-[^{131}I]IB-D-EEEG or Mal-D-GEEEK-[^{125}I]IB. With the caveat that different cell lines were used, this suggests that negatively charged D-amino acid peptide templates offer the possibility of achieving at least comparable levels of residualization as is possible with radiometals.

3.4. Biodistribution in mice with BT474M1 xenografts

The tissue distribution of trastuzumab-NHS-[^{131}I]IB-D-EEEG and trastuzumab-Mal-D-GEEEK-[^{125}I]IB was compared in a paired-label format in athymic mice bearing subcutaneous BT474M1 xenografts. The HER2-expressing BT474M1 cell line [32], a metastatic variant of the BT474 cell line, was used for xenotransplantation due to its increased tumorigenicity [33]. The percentage of the injected dose of radioiodine activity per gram (%ID/g) present in normal tissues as a function of time is presented in Table 1. Accumulation of both radionuclides showed a similar pattern in most tissues. Radioiodine levels in stomach and thyroid (%/organ) were low indicating a low susceptibility towards *in vivo* deiodination for both conjugates; however, at later time points, the NHS-[^{131}I]IB-D-EEEG-mAb conjugate exhibited significantly lower uptake ($P < 0.05$) in these tissues that are known to accumulate free iodide. The most striking differences observed in the biodistribution of the two D-peptide-trastuzumab conjugates were observed in tumor and kidneys (Fig. 3). Unlike the binding affinity, immunoreactivity and internalization behavior seen in the *in vitro* experiments with BT474 cells, BT474M1 xenograft accumulation of trastuzumab-NHS-[^{131}I]IB-D-EEEG was about 1.2–1.5 times lower than that of co-administered trastuzumab-Mal-D-GEEEK-[^{125}I]IB at all time-points. Given the similarity in the *in vitro* behavior of the two radioiodinated trastuzumab conjugates, it seems possible that the lower uptake of radioactivity in tumor from trastuzumab-NHS-[^{131}I]IB-D-EEEG could have been due to differential metabolism of the two tracers.

Nonetheless, the tumor uptake observed for both radioconjugates was relatively high, reaching a maximum of 29.8% ± 3.6% ID/g for trastuzumab-NHS-[^{131}I]IB-D-EEEG and 45.3% ± 5.3% ID/g for trastuzumab-Mal-D-GEEEK-[^{125}I]IB at 48 h. In comparison, the BT474 xenograft uptake reported for trastuzumab labeled with ^{99m}Tc-tricarbonyl [34], ^{188}Re-tricarbonyl [35], or ^{188}Re-SOCTA [22] was considerably lower, at 8.2% ± 1.6% ID/g, 16.9% ± 5.4% ID/g and 7.3% ± 1.2% ID/g, respectively at 48 h. Although comparisons with studies done in different tumor models must be done with caution, the peak tumor uptakes observed for the two D-peptide-trastuzumab conjugates in the current study also compared favorably with the results obtained with radiolabeled trastuzumab preparations evaluated in other HER2-expressing tumor models. With regard to other radioiodination approaches, the maximum tumor uptake reported for trastuzumab labeled using *N*-succinimidyl *p*-[^{125}I] iodobenzoate was about 16% ID/g at 24 h in NCI-N87 gastric adenocarcinoma xenografts [28]. In three studies performed in the SKOV-3 ovarian carcinoma model with trastuzumab labeled with ^{111}In using residualizing DTPA-derivatives as chelating agents, the tumor uptake levels observed at 24 h were 13.7% ± 0.6% ID/g [31], 17.7% ± 1.9% ID/g [36] and about 20% ID/g [37]. Finally, in a recent study also performed in mice with SKOV-3 xenografts, tumor uptake for trastuzumab labeled with ^{111}In and ^{177}Lu labeled *via* the

Table 1
Paired-label biodistribution of trastuzumab labeled with NHS-[^{131}I]IB-D-EEEG and Mal-D-GEEEK-[^{125}I]IB in athymic mice bearing subcutaneous BT474M1 human breast carcinoma xenografts.

Organ/Tissue	%ID/g [a]					
	4 h	12 h	24 h	48 h	96 h	144 h
Iodine-131						
Liver	12.87 ± 1.53	5.40 ± 0.72	4.68 ± 0.61	3.53 ± 0.24	2.44 ± 0.65	1.28 ± 0.26
Spleen	21.94 ± 5.32	11.92 ± 3.31	11.37 ± 2.63	7.89 ± 0.58	5.54 ± 2.51	2.54 ± 1.01
Lungs	10.45 ± 1.95	5.53 ± 0.42	5.08 ± 0.41	4.03 ± 0.40	3.28 ± 1.18	1.70 ± 0.51[b]
Heart	6.69 ± 1.08	3.60 ± 1.11	3.01 ± 0.52	2.38 ± 0.49	1.73 ± 0.63	0.93 ± 0.33[b]
Stomach	1.55 ± 0.74	1.23 ± 0.13	1.43 ± 0.38	1.11 ± 0.33	0.55 ± 0.17	0.31 ± 0.09
Small intestine	2.77 ± 0.49	1.71 ± 0.19	1.70 ± 0.36	1.28 ± 0.06	0.87 ± 0.26	0.43 ± 0.10
Large intestine	2.65 ± 0.21[b]	1.92 ± 0.42[b]	1.83 ± 0.43	1.60 ± 0.45	0.81 ± 0.33	0.53 ± 0.26
Thyroid	0.60 ± 0.19[b]	0.32 ± 0.12	0.41 ± 0.15	0.29 ± 0.07	0.19 ± 0.12	0.12 ± 0.03[b]
Muscle	1.30 ± 0.26	1.25 ± 0.19	1.21 ± 0.14	0.96 ± 0.15	0.67 ± 0.16	0.33 ± 0.11[b]
Blood	21.92 ± 6.42	10.92 ± 1.45	10.04 ± 0.59	7.55 ± 0.96	5.68 ± 2.07	2.72 ± 0.75[b]
Bone	2.41 ± 0.38	1.49 ± 0.16	1.47 ± 0.20	1.17 ± 0.19	0.79 ± 0.22	0.42 ± 0.14
Brain	0.74 ± 0.11	0.35 ± 0.06	0.34 ± 0.03	0.27 ± 0.03	0.21 ± 0.08	0.10 ± 0.02[b]
Iodine-125						
Liver	13.25 ± 1.60	6.45 ± 0.91	5.72 ± 0.67	4.53 ± 0.49	3.15 ± 0.59	1.76 ± 0.39
Spleen	25.83 ± 6.27	14.00 ± 3.78	13.47 ± 3.21	10.03 ± 0.61	7.21 ± 2.88	3.54 ± 1.09
Lungs	12.00 ± 2.29	6.49 ± 0.55	6.32 ± 0.59	4.88 ± 0.50	3.62 ± 1.33	1.67 ± 0.58
Heart	7.63 ± 1.25	4.18 ± 1.22	3.57 ± 0.64	2.81 ± 0.52	1.91 ± 0.73	0.92 ± 0.34
Stomach	1.68 ± 0.81	1.60 ± 0.13	1.92 ± 0.57	1.53 ± 0.37	0.76 ± 0.21	0.39 ± 0.12
Small intestine	3.04 ± 0.56	1.97 ± 0.18	2.00 ± 0.44	1.55 ± 0.09	1.02 ± 0.30	0.48 ± 0.11
Large intestine	2.51 ± 0.43	2.23 ± 0.48	1.89 ± 0.41	1.96 ± 0.58	1.04 ± 0.47	0.64 ± 0.30
Thyroid	0.64 ± 0.22	0.37 ± 0.12	0.50 ± 0.18	0.44 ± 0.09	0.51 ± 0.25	0.49 ± 0.19
Muscle	1.54 ± 0.34	1.43 ± 0.23	1.45 ± 0.17	1.15 ± 0.17	0.74 ± 0.17	0.33 ± 0.11
Blood	24.88 ± 7.22	12.41 ± 1.54	11.84 ± 0.77	8.89 ± 1.18	6.42 ± 2.53	2.76 ± 0.90
Bone	2.79 ± 0.51	1.72 ± 0.14	1.83 ± 0.22	1.48 ± 0.19	0.97 ± 0.28	0.58 ± 0.19
Brain	0.85 ± 0.13	0.40 ± 0.07	0.41 ± 0.03	0.32 ± 0.03	0.24 ± 0.10	0.10 ± 0.02

[a] Values are mean %ID/g ± SD (n = 5) except for thyroid which %ID/organ is used.
[b] No significant difference between the two tracers ($P > 0.05$).

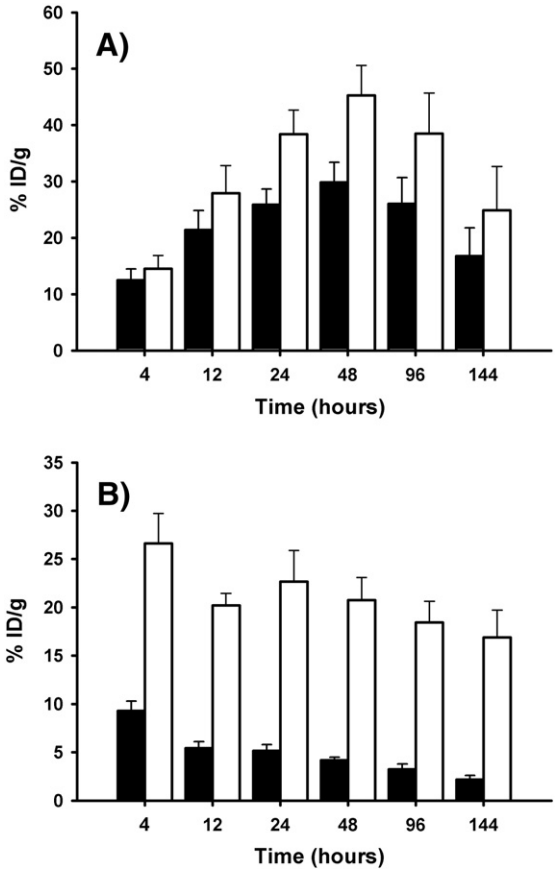

Fig. 3. Paired-label uptake in athymic mice with BT474M1 xenografts of trastuzumab-NHS-[^{131}I]IB-D-EEEG (closed bars) and trastuzumab-Mal-D-GEEEK-[^{125}I]IB (open bars) in tumor (A) and kidney (B).

DOTA macrocycle was comparable to that measured in the current study but lower than that obtainable (^{111}In, 58.3% ± 17.2% ID/g; ^{177}Lu, 63.5% ± 15% ID/g at 48 h) with the newly described acyclic chelator, H_4octapa [38].

A potential disadvantage observed in previous studies evaluating the possible utility of Mal-D-GEEEK-[*I]IB for protein radioiodination is that kidney radioactivity levels were higher than those resultant from the use of other labeling strategies. These differences were most striking with 15 kDa nanobodies [18,23], in the protein size range characterized by having high renal tubular reabsorption [39]; however, even with 150 kDa intact mAbs [15] and a 105 kDa mAb fragment [16], kidney activity levels were two-to threefold higher after Mal-D-GEEEK-[*I]IB labeling compared with direct electrophilic protein iodination. A possible explanation for this behavior which has been proposed [16] is that Mal-D-GEEEK-[*I]IB contains three glutamic acid residues that might be recognized by the EAAT3 transporter, which facilitates proximal tubular reabsorption of L-glutamic acid [40]. However, the results of the current study contradict this hypothesis because kidney levels for trastuzumab-NHS-[^{131}I]IB-D-EEEG were significantly lower ($P < 0.0003$) than those for trastuzumab-Mal-D-GEEEK-[^{125}I]IB at all time points (Fig. 3) even though both acylation agents contain three D-glutamic acid residues. For example, kidney uptake after Mal-D-GEEEK-[^{125}I]IB labeling at 4 h was 26.6% ± 3.1% ID/g compared with 9.3% ± 1.0% ID/g for NHS-[^{131}I]IB-D-EEEG, with the difference increasing with time, up to a factor of 8 at 144 h (16.9% ± 2.8% ID/g *vs* 2.2% ± 0.4% ID/g).

The significantly lower kidney uptake and expedited renal clearance observed with NHS-[*I]IB-D-EEEG labeling could be advantageous in reducing renal radiation dose, particularly for targeted radiotherapy, and for imaging HER2-expressing cancers in close proximity to the kidneys. It remains to be ascertained whether similar advantages will be obtainable with smaller proteins such as nanobodies, where kidney levels in excess of 100% ID/g were observed after labeling with Mal-D-GEEEK-[*I]IB [18,23]. The mechanisms responsible for the differential kidney uptake of proteins labeled

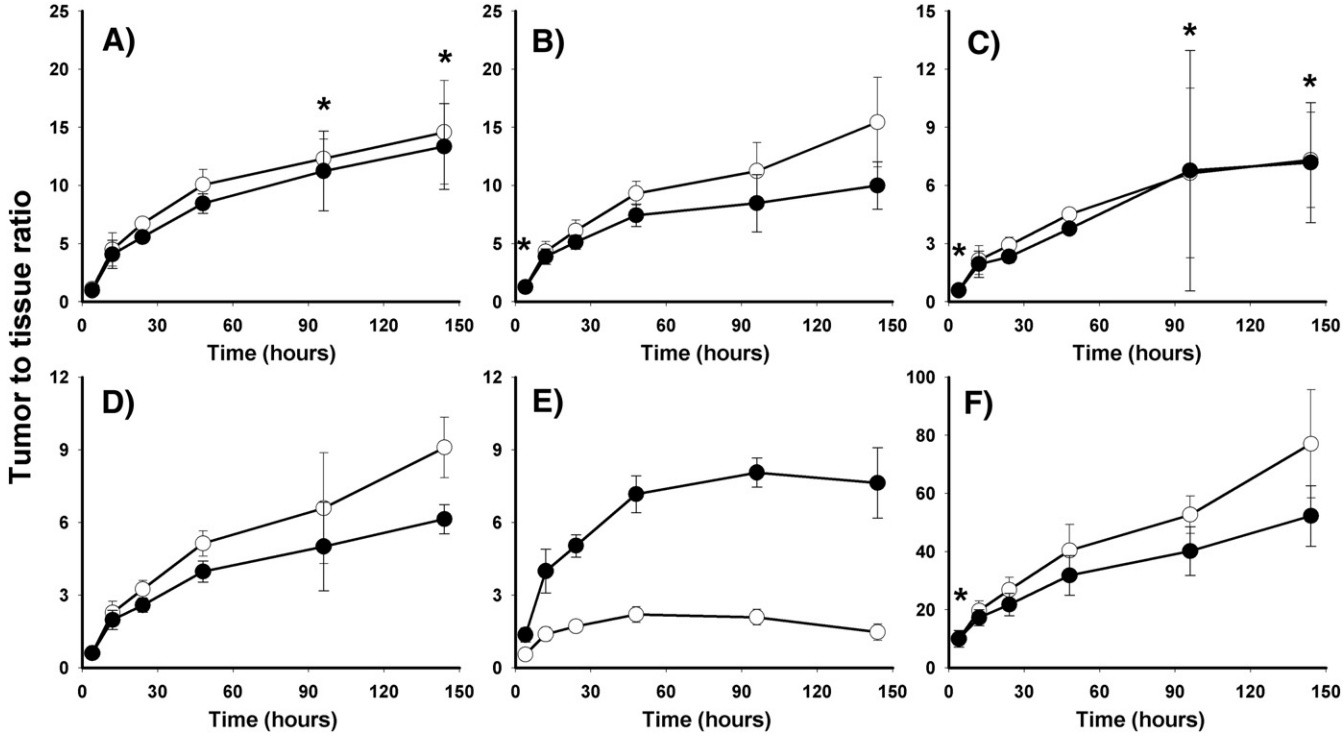

Fig. 4. Tumor-to-normal tissue ratios in athymic mice bearing BT474M1 xenografts for trastuzumab labeled with NHS-[^{131}I]IB-D-EEEG (filled circles) and Mal-D-GEEEK-[^{125}I]IB (open circles): liver (A), lungs (B), spleen (C), blood (D), kidneys (E), muscle (F). *No significant difference between the two tracers ($P > 0.05$).

with these (D-glutamic acid)$_3$-bearing peptide-[*I]iodobenzoyl conjugate residualization agents are not known at this time. To address this question, we plan to perform extensive analyses of labeled catabolites generated *in vivo* from proteins with molecular weights above and below the cutoff for renal filtration after labeling with NHS-[*I]IB-D-EEEG and Mal-D-GEEEK-[*I]IB.

The final parameter utilized for evaluation of the potential utility of the two D-peptide based residualization agents for labeling trastuzumab was the ratio of activity localized in tumor to that observed in normal tissue. As summarized in Fig. 4, tumor-to-normal tissue (T/NT) ratios for trastuzumab-Mal-D-GEEEK-[^{125}I]IB were the same or slightly higher than those obtained for trastuzumab-NHS-[^{131}I]IB-D-EEEG for most tissues except kidneys. Tumor-to-kidney ratios observed with NHS-[^{131}I]IB-D-EEEG were 2.5 times higher than those seem with Mal-D-GEEEK-[^{125}I]IB at 4 h with the difference increasing to a factor of 5 by 6 days post injection. The tumor-to-normal tissue ratios measured for trastuzumab-NHS-[^{131}I]IB-D-EEEG and trastuzumab-Mal-D-GEEEK-[^{125}I]IB compared favorably with those for trastuzumab labeled with *N*-succinimidyl *p*-[^{125}I]iodobenzoate [28], which has the same dehalogenation resistant template as these D-peptide reagents, but lacks functionalities designed for intracellular trapping.

4. Conclusions

A new radiohalogenation agent, NHS-[*I]IB-D-EEEG, analogous to previously developed Mal-D-GEEEK-[*I]IB, was synthesized and conjugated in reasonable yields to an internalizing mAb trastuzumab. Although, the yield for coupling NHS-[*I]IB-D-EEEG to trastuzumab was somewhat lower than that for Mal-D-GEEEK-[*I]IB, the whole procedure was simpler and faster, which could be particularly important for use with short-lived radiohalogens such as ^{123}I and ^{211}At. Although intracellular retention of radioiodine in HER2-expressing breast cancer cells *in vitro* occurred at similar high levels with both labeling methods, retention of radioactivity in BT474M1 xenografts was about 20%–50% lower when mAb was labeled using NHS-[*I]IB-D-EEEG. On the other hand, tumor-to-normal tissues ratios were similar for both labeling methods and in kidneys were significantly higher when the new reagent was used. Future studies are planned to evaluate the *in vivo* catabolism of mAbs labeled *via* these D-peptide based reagents with the goal of identifying structural components that will allow the best balance for maximizing tumor uptake while minimizing kidney retention not only for intact mAbs but also for smaller mAb fragments including nanobodies.

Acknowledgments

This work was supported in part by Grants CA42324 and CA154291 from the National Institutes of Health. The technical assistance of Dr. Xiao-Guang Zhao with the biodistribution experiments is greatly appreciated.

References

[1] Scholl S, Beuzeboc P, Pouillart P. Targeting HER2 in other tumor types. Ann Oncol 2001;12(Suppl. 1):S81–7.
[2] Baselga J. Clinical trials of Herceptin (trastuzumab). Eur J Cancer 2001;37(Suppl 1): S18–24.
[3] Agus DB, Gordon MS, Taylor C, Natale RB, Karlan B, Mendelson DS, et al. Phase I clinical study of pertuzumab, a novel HER dimerization inhibitor, in patients with advanced cancer. J Clin Oncol 2005;23:2534–43.
[4] Blackwell KL, Burstein HJ, Storniolo AM, Rugo HS, Sledge G, Aktan G, et al. Overall survival benefit with lapatinib in combination with trastuzumab for patients with human epidermal growth factor receptor 2-positive metastatic breast cancer: final results from the EGF104900 Study. J Clin Oncol 2012;30:2585–92.
[5] Akabani G, Carlin S, Welsh P, Zalutsky MR. In vitro cytotoxicity of ^{211}At-labeled trastuzumab in human breast cancer cell lines: effect of specific activity and HER2 receptor heterogeneity on survival fraction. Nucl Med Biol 2006;33:333–47.
[6] Persson M, Gedda L, Lundqvist H, Tolmachev V, Nordgren H, Malmström PU, et al. [^{177}Lu]pertuzumab: experimental therapy of HER-2-expressing xenografts. Cancer Res 2007;67:326–31.
[7] Ray GL, Baidoo KE, Keller LMM, Albert PS, Brechbiel MW, Milenic DE. Pre-clinical assessment of ^{177}Lu-labeled trastuzumab targeting HER2 for treatment and management of cancer patients with disseminated intraperitoneal disease. Pharmaceuticals 2012;5:1–15.
[8] McLarty K, Cornelissen B, Cai Z, Scollard DA, Costantini DL, Done SJ, et al. Micro-SPECT/CT with ^{111}In-DTPA-pertuzumab sensitively detects trastuzumab-mediated HER2

downregulation and tumor response in athymic mice bearing MDA-MB-361 human breast cancer xenografts. J Nucl Med 2009;50:1340–8.
[9] Holloway CM, Scollard DA, Caldwell CB, Ehrlich L, Kahn HJ, Reilly RM. Phase I trial of intraoperative detection of tumor margins in patients with HER2-positive carcinoma of the breast following administration of ^{111}In-DTPA-trastuzumab Fab fragments. Nucl Med Biol 2013;40:630–7.
[10] Geissler F, Anderson SK, Press O. Intracellular catabolism of radiolabeled anti-CD3 antibodies by leukemic T cells. Cell Immunol 1991;137:96–110.
[11] Garg S, Garg PK, Zalutsky MR. *N*-succinimidyl-5-(trialkylstannyl)-3-pyridinecarboxylates: a new class of reagents for protein radioiodination. Bioconjug Chem 1991;2:50–6.
[12] Foulon CF, Reist CJ, Bigner DD, Zalutsky MR. Radioiodination via D-amino acid peptide enhances cellular retention and tumor xenograft targeting of an internalizing anti-epidermal growth factor receptor variant III monoclonal antibody. Cancer Res 2000;60:4453–60.
[13] Shankar S, Vaidyanathan G, Affleck D, Welsh PC, Zalutsky MR. *N*-succinimidyl 3-[^{131}I]iodo-4-phosphonomethylbenzoate ([^{131}I]SIPMB), a negatively charged substitutent-bearing acylation agent for the radioiodination of peptides and mAbs. Bioconjug Chem 2003;14:331–41.
[14] Vaidyanathan G, Affleck DJ, Li J, Welsh P, Zalutsky MR. A polar substituent-containing acylation agent for the radioiodination of internalizing monoclonal antibodies: *N*-succinimidyl 4-guanidinomethyl-3-[^{131}I]iodobenzoate ([^{131}I]SGMIB). Bioconjug Chem 2001;12:428–38.
[15] Vaidyanathan G, Alston KL, Bigner DD, Zalutsky MR. N^{ε}-(3-[*I]iodobenzoyl)-Lys^5-N^{α}-maleimido-Gly^1-GEEEK ([*I]IB-Mal-D-GEEEK): a radioiodinated prosthetic group containing negatively charged D-glutamates for labeling internalizing monoclonal antibodies. Bioconjug Chem 2006;17:1085–92.
[16] Vaidyanathan G, Jestin E, Olafsen T, Wu AM, Zalutsky MR. Evaluation of an anti-p185^{HER2} (scFv-C_H2-C_H3)$_2$ fragment following radioiodination using two different residualizing labels: SGMIB and IB-Mal-D-GEEEK. Nucl Med Biol 2009;36:671–80.
[17] Vaidyanathan G, White BJ, Affleck DJ, Zhao XG, Welsh PC, McDougald D, et al. SIB-DOTA: a trifunctional prosthetic group potentially amenable for multi-modal labeling that enhances tumor uptake of internalizing monoclonal antibodies. Bioorg Med Chem 2012;20:6929–39.
[18] Pruszynski M, Koumarianou E, Vaidyanathan G, Revets H, Devoogdt N, Lahoutte T, et al. Targeting breast carcinoma with radioiodinated anti-HER2 Nanobody. Nucl Med Biol 2013;40:52–9.
[19] Hermanson GT. Bioconjugate techniques. 2nd ed. Amsterdam: Academic Press; 2008.
[20] Zalutsky MR, Narula AS. A method for the radiohalogenation of proteins resulting in decreased thyroid uptake of radioiodine. Appl Radiat Isot 1987;38:1051–5.
[21] Vaidyanathan G, Zalutsky MR. Protein radiohalogenation: observations on the design of *N*-succinimidyl ester acylation agents. Bioconjug Chem 1990;1:269–73.
[22] Luo TY, Tang IC, Wu YL, Hsu KL, Liu SW, Kung HC, et al. Evaluating the potential of ^{188}Re-SOCTA-trastuzumab as a new radioimmunoagent for breast cancer treatment. Nucl Med Biol 2009;36:81–8.
[23] Pruszynski M, Koumarianou E, Vaidyanathan G, Revets H, Devoogdt N, Lahoutte T, et al. Improved tumor targeting of anti-HER2 nanobody through *N*-succinimidyl 4-guanidinomethyl-3-iodobenzoate radiolabeling. J Nucl Med 2014;55:650–6.
[24] Whetstone PA, Akizawa H, Meares CF. Evaluation of cleavable (Tyr^3)-octreotate derivatives for longer intracellular probe residence. Bioconjug Chem 2004;15:647–57.
[25] Jaramillo ML, Leon Z, Grothe S, Paul-Roc B, Abulrob A, O'Connor McCourt M. Effect of the anti-receptor ligand-blocking 225 monoclonal antibody on EGF receptor endocytosis and sorting. Exp Cell Res 2006;312:2778–90.
[26] Austin CD, De Mazière AM, Pisacane PI, van Dijk SM, Eigenbrot C, Sliwkowski MX, et al. Endocytosis and sorting of ErbB2 and the site of action of cancer therapeutics trastuzumab and geldanamycin. Mol Biol Cell 2004;15:5268–82.
[27] Orlova A, Bruskin A, Sivaev I, Sjöberg S, Lundqvist H, Tolmachev V. Radio-iodination of monoclonal antibody using potassium [^{125}I]-(4-isothiocyanatobenzylammonio)-iodo-decahydro-*closo*-dodecaborate (iodo-DABI). Anticancer Res 2006;26:1217–24.
[28] Orlova A, Wållberg H, Stone-Elander S, Tolmachev V. On the selection of a tracer for PET imaging of HER2-expressing tumors: direct comparison of a ^{124}I-labeled affibody molecule and trastuzumab in a murine xenograft model. J Nucl Med 2009;50:417–25.
[29] Persson MI, Gedda L, Jensen HJ, Lundqvist H, Malmström PU, Tolmachev V. Astatinated trastuzumab, a putative agent for radionuclide immunotherapy of ErbB2-expressing tumours. Oncol Rep 2006;15:673–80.
[30] Shih LB, Thorpe SR, Griffiths GL, Diril H, Ong GL, Hansen HJ, et al. The processing and fate of antibodies and their radiolabels bound to the surface of tumor cells in vitro: a comparison of nine radiolabels. J Nucl Med 1994;35:899–908.
[31] Lub-de Hooge MN, Kosterink JGW, Perik PJ, Nijnuis H, Tran L, Bart J, et al. Preclinical characterisation of ^{111}In-DTPA-trastuzumab. Br J Pharmacol 2004;143:99–106.
[32] Beyer I, Li Z, Persson J, Liu Y, van Rensburg R, Yumul R, et al. Controlled extracellular matrix degradation in breast cancer tumors improves therapy by trastuzumab. Mol Ther 2011;19:479–89.
[33] Nielsen UB, Kirpotin DB, Pickering EM, Hong K, Park JW, Refaat Shalaby M, et al. Therapeutic efficacy of anti-ErbB2 immunoliposomes targeted by a phage antibody selected for cellular endocytosis. Biochim Biophys Acta 2002;1591:109–18.
[34] Yen CL, Chen WJ, Lo ST, Chen KT, Yao CL, Lee TW, et al. Biodistribution of Tc-99 m (I)-tricarbonyl labeled trastuzumab as an imaging agent for breast cancer with HER2 overexpression in an animal model. Ann Nucl Med Mol Imaging 2011;24:119–22.
[35] Chen KT, Lee TW, Lo JM. In vivo examination of ^{188}Re(I)-tricarbonyl-labeled trastuzumab to target HER2-overexpressing breast cancer. Nucl Med Biol 2009;36:355–61.
[36] Dijkers ECF, Kosterink JGW, Rademaker AP, Perk LR, van Dongen GAMS, Bart J, et al. Development and characterization of clinical-grade ^{89}Zr-trastuzumab for HER2/*neu* immunoPET imaging. J Nucl Med 2009;50:974–81.
[37] Milenic DE, Wong KJ, Baidoo KE, Nayak TK, Regino CAS, Garmestani K, et al. Targeting HER2. A report on the in vitro and in vivo pre-clinical data supporting trastuzumab as a radioimmunoconjugate for clinical trials. MAbs 2010;2:550–64.
[38] Price EW, Zeglis BM, Cawthray JF, Ramogida CF, Ramos N, Lewis JS, et al. H_4octapa-trastuzumab: versatile acyclic chelate system for ^{111}In and ^{177}Lu imaging and therapy. J Am Chem Soc 2013;135:12707–21.
[39] Vegt E, de Jong M, Wetzels JFM, Masereeuw R, Melis M, Oyen WJG, et al. Renal toxicity of radiolabeled peptides and antibody fragments: mechanisms, impact on radionuclide therapy, and strategies for prevention. J Nucl Med 2010;51:1049–58.
[40] Verrey F, Ristic Z, Romeo E, Ramadan T, Makrides V, Dave MH, et al. Novel renal amino acid transporters. Annu Rev Physiol 2005;67:557–72.